

Proceeding Paper

# Manufacturing and Testing of 3D-Printed Polymer Isogrid Lattice Cylindrical Shell Structures <sup>†</sup>

César M. A. Vasques <sup>\*ID</sup>, Fernando C. Gonçalves <sup>ID</sup> and Adélio M. S. Cavadas

proMetheus, Escola Superior de Tecnologia e Gestão, Instituto Politécnico de Viana do Castelo, Rua Escola Industrial e Comercial de Nun'Álvares, 4900-347 Viana do Castelo, Portugal; fegs@ipvc.pt (F.C.G.); adelioc@estg.ipvc.pt (A.M.S.C.)

\* Correspondence: cmavasques@gmail.com

† Presented at the 2nd International Electronic Conference on Applied Sciences, 15–31 October 2021; Available online: <https://asec2021.sciforum.net>.

**Abstract:** This article focuses on the use of fused deposition modeling (FDM) technology to manufacture and test polymer isogrid lattice cylindrical shell (LCS) structures with equilateral triangular unit-cells using non-professional and conventional 3D printing software and hardware. A parametric and automated 3D model for these structures is created in SolidWorks using the Visual Basic (VBA) programming language. Different configurations of the isogrid LCS structure are modeled, manufactured, and tested in order to determine the compressive structural strength and stiffness, as well as to investigate structural instability. The experimental results are used to deduce the inherent limitations of 3D printing, including the inhomogeneities, imperfections, and non-isotropic nature of FDM, as well as the effect of the configurations on local buckling behavior. The results suggest that coupling between local and global buckling has an impact on the compressive stiffness and strength of LCS structures, reducing the accuracy of structural designs neglecting these effects.

**Keywords:** isogrid; cylindrical shell; polymer structures; additive manufacturing; fused deposition modeling; 3D printing; local buckling



**Citation:** Vasques, C.M.A.;

Gonçalves, F.C.; Cavadas, A.M.S.

Manufacturing and Testing of  
3D-Printed Polymer Isogrid Lattice  
Cylindrical Shell Structures. *Eng.  
Proc.* **2021**, *11*, 47. [https://doi.org/  
10.3390/ASEC2021-11174](https://doi.org/10.3390/ASEC2021-11174)

Academic Editor: Filippo Berto

Published: 15 October 2021

**Publisher's Note:** MDPI stays neutral  
with regard to jurisdictional claims in  
published maps and institutional affil-  
iations.



**Copyright:** © 2021 by the authors.  
Licensee MDPI, Basel, Switzerland.  
This article is an open access article  
distributed under the terms and  
conditions of the Creative Commons  
Attribution (CC BY) license ([https://  
creativecommons.org/licenses/by/  
4.0/](https://creativecommons.org/licenses/by/4.0/)).

## 1. Introduction

Lattice cylindrical shell (LCS) structures have been applied in a wide variety of fields, from aerospace to medicine, and are now recognized as a viable design alternative for critical geodesic structural applications requiring lightweight, low-cost structures with high mechanical performance. Lattice structures are typically used as reinforcements for homogeneous shells, such as aerial aircraft fuselage sections, or as standalone structures that perform critical functions, such as stent devices [1–4]. In general, these structures combine axial, circumferential, and helical ribs to increase the strength-to-mass ratio of cylinder shells when subjected to axial, bending, and torsion stresses [5–7].

Different approaches to designing, developing, and manufacturing these lightweight structures have been pursued in different countries since McDonnell–Douglas and NASA first idealized and consolidated the isogrid concept for metallic aerospace structures in the 1970s in the United States [1,8]; these lightweight structures were indeed manufactured by first machining in the flat and then forming. Their design and manufacturing were extended in the 1980s by CRISM in the former Soviet Union to the so-called *anisogrid* (in relation with the anisotropy of composite materials) design concept, which, instead, considered composite carbon-fiber materials and LCS structures formed via filament winding. Due to the manufacturing constraints and disadvantages of metallic isogrid LCS structures, several studies on more general composite anisogrid geodesic designs have been conducted, covering design [9–11], manufacturing [12], mechanical properties [13], buckling [5], failure [14], and applications [2,15–18], to name only a few. Structural models of the lattice may be simplified by “smearing out”, averaging, or taking mean values of the

lattice properties and considering them as a solid continuous sheet of isotropic material with elastic properties [8,19–22]. Alternatively, more precise but more complex approaches may be used in conjunction with finite element technology, when using numerical computational analysis tools [5,6,21,23]. In the case of metallic lattices, the term *isogrid* has been used because the structure has been originally assumed to behave like an isotropic material [8], but recent studies appear to indicate otherwise [24].

Numerous LCS topologies can be created by varying the number of ribs and their arrangement, including the typical hexagonal, triangular, and mixed grid lattice shells [6,22]. Due to their complexity in terms of geometry definition, model generation, and physical realization, these structures pose significant design and manufacturing challenges, for which the increased creativity and design freedom enabled by additive manufacturing (AM) and 3D printing technologies are extremely beneficial, with potential to rapidly transform the engineering of lattice structures as we classically know it. Nowadays, AM is a widely used manufacturing process in which critical build-up parts are manufactured by layering or fusing materials in accordance with precise computerized 3D solid digital models. As such, new disruptive design and manufacturing paradigms are emerging, characterized by increased design flexibility and optimization, manufacturing simplicity, product customization, and degree of automation, where numerous remarkable technologies are converging at the moment: intelligent software, novel materials, novel manufacturing processes (particularly 3D printing and AM), robotics and automation, and a slew of web-based services. Additionally, freely available and widely disseminated computer-aided design (CAD) and manufacturing (CAM) software, as well as the well established computer numerical control (CNC) standards, combined with readily available and affordable commercial 3D printers and materials, have fostered a boom in the number of users and potential applications for these technologies. In the context of lattice structures, recent attention has been focused on both metal [25–30] and polymer [31–35] 3D printed parts for a variety of different applications and purposes (cf. also the review works in [36,37] and the references therein), most commonly limited to multipurpose planar designs or volumetric lightweight cellular structural infills.

This work is based on a preliminary investigation conducted as part of an undergraduate mechanical engineering student's final project motivated by Vasiliev and Totaro's advancements in composite LCS structures fabricated with the filament winding process [2,10,15,16,23]. While the latter studies are fascinating and instructive, they are limited to composite materials and filament winding processes on large-scale structures, rendering them inaccessible to the general public, where large-scale testing is also more challenging. With the advancement of 3D printing technologies and the availability of new materials and large-format printing underway, we are on the verge of witnessing a paradigm shift in lattice structure engineering that will enable greater design flexibility and physical realization, circumventing the primary limitations of filament winding composites.

As such, the overall goal of this work is to provide a first step and experimental contribution toward a better understanding of the feasibility of 3D-printed isogrid LCS structures at a small scale and to assess their local buckling mechanics through testing. In summary, this article starts by describing a 3D geometric model of isogrid LCS structures with a unit equilateral triangular cell that enables automatic generation of various configurations in SolidWorks. Next, polymer isogrid LCS structural test samples are fabricated using fused deposition modeling (FDM) and mechanically tested to determine the LCS structure's strength, stiffness, and mode of failure during buckling. While 3D printing by FDM introduces uncertainty regarding material properties and homogeneity by introducing some degree of anisotropy, it also simplifies analysis by utilizing smaller-scale, more affordable, and manageable polymer isogrid LCS structural samples. Furthermore, despite the focus being on the use of an accessible and affordable FDM technology and 3D printing software and hardware to manufacture cylindrical shell structures with equilateral triangular unit cells via 3D printing and on the study of local buckling, more refined and professional systems may be used to make the process more reliable, scalable, and applica-

ble to large-formats and high-performance engineering materials. Lastly, the article ends with a summary of the most important findings and conclusions.

## 2. Geometry and 3D Modeling

An *isogrid* is an array of continuous equilateral triangles formed by a lattice of stiffening ribs; it is the simplest arrangement of bar elements with isotropic properties, hence the name. The intersecting ribs form a complete lattice (or grid) structure, regardless of whether they are attached to a single (or doubled) skin or used as an open lattice. The isogrid lattice's ability to control stresses via the ribs enables it to replace traditional solid structural elements with equivalent lattice shapes, thereby reducing weight and increasing mechanical strength. Despite their structural efficiency, these structures are still being investigated using novel materials and lattice morphologies. The morphology used in this study is the same as that used by Vasiliev and Totaro [16,23] for isogrid geodesic shells, which is defined by a cylindrical shell structure without skin (also typically ignored in design for load bearing), with ribs forming triangular unit cells patterned in the geodesic surface of the LCS structure. This morphology is comparable to that of an isotropic material shell structure and typically results in a combination of compression and tensile stresses in the ribs under general loading. As shown in Figure 1, seven parameters were considered to completely define the full LCS geometry, namely the LCS external diameter,  $D$ , and length,  $L$ ; the constant width of the ribs on the tangent plane,  $a$ , and along the radial direction,  $e$ ; the number of helical and circumferential ribs,  $n_h$  and  $n_c$ , respectively (no axial ribs are necessary for this unit cell orientation and morphology without vertical sides); and the height  $h$  of each stage in between two successive circumferential ribs. Of these, only five parameters are actually independent and required for its modeling; for example, we have considered the height  $h$  and length  $L$  as the dependent parameters and the remainder as the independent ones.

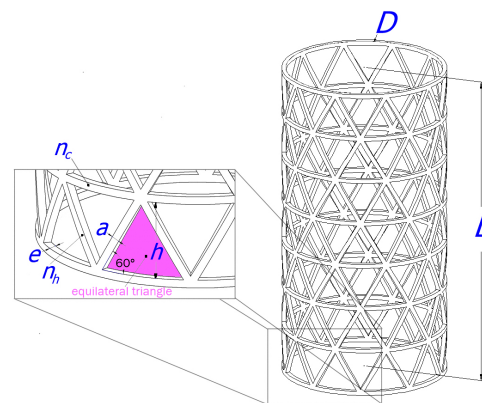


**Figure 1.** Geometric parameters required to fully define the 3D model of the isogrid LCS structure.

The geometry was chosen to favor local instability phenomena such as local buckling by having a low density of equilateral triangular unit cells and shells with a low total length-to-diameter ratio. Due to practical and manufacturing constraints, such as the printing volume and filament diameter of conventional polymer FDM 3D printing systems, small-scale samples can be printed with sufficient representativeness for a small number of unit cells only if the interrelated parameters of maximum diameter, number of circumferential ribs, and width are properly adjusted, thus precluding the analysis of global buckling. Considering previous works [15,23] and structural stability theory, the geometry was chosen to favor the appearance of local rib buckling along the tangential circumferential (as opposed to radial) axis of the cylinder (ensuring that  $e > a$ ) and establishing a distance between circumferential ribs that ensures the application of Euler's column formula [38] for the determination of the critical rib buckling load, as well as an appropriate rib slenderness ratio that ensures the critical Euler stress is less than half the material's yield stress. As such,

once the material properties and internal loads are known, Euler’s buckling theory can be used to approximate the local buckling critical load by treating the ribs as beams. This approach, however, may be oversimplified, as complicating effects such as those caused by the inherent material anisotropy of FDM 3D printing, border effects at loaded extremity faces, border effects and stress distributions at rib junctions in the triangle vertices, and those caused by the LCS structure’s global deformation behavior in compression complicate the analysis. These key aspects will be partially examined in better detail in the sections that follow and ongoing work.

The isogrid LCS structure’s geometry is created parametrically and automatically in SolidWorks, allowing models to be created with minimal effort and in the shortest amount of time possible, thereby optimizing the design cycle. The required parameters input, operations, and graphical user interface (GUI) were programmed in Visual Basic (VBA) and made available as a button in the SolidWorks environment, as well as a GUI pop-up that appears when necessary as depicted in Figure 2.

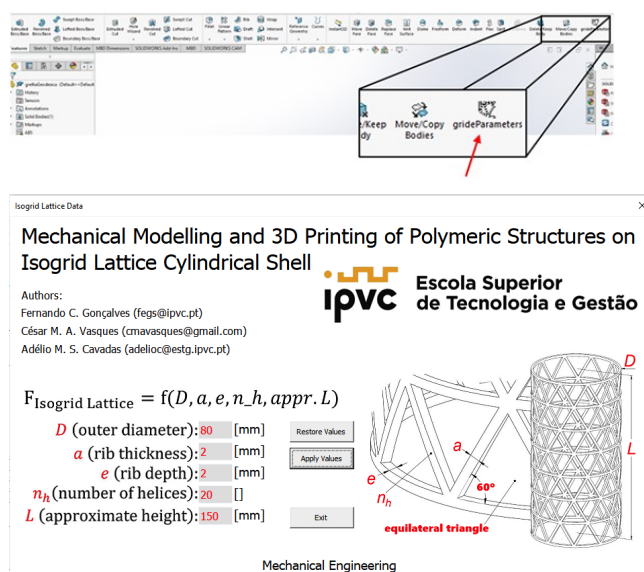


**Figure 2.** Graphical user interface used to introduce the parameters to automatically build the geometric 3D model of the isogrid LCS in SolidWorks and dedicated call-up button integrated into the SolidWorks environment workspace.

In a first stage, the geometry was designed in SolidWorks to ensure minimal operations and a clear understanding of how the geometry could be constructed. From there, complications arose when attempting to identify the internal variables that SolidWorks assigns to each operation and each parameter of each operation during the interface’s VBA programming. This interface provides aids and easy visual identification for each parameter, as well as a friendly environment in which the user can enter the input data. Existing warnings and error messages assist in rectifying incorrectly entered values. To facilitate integration with SolidWorks, the VBA interface was inserted into the SolidWorks environment as illustrated. The VBA program’s overall functional rationale is to automatically modify an existing geometry based on new desired parameters, where the user initially sees an example structure.

### 3. Manufacturing and 3D Printing

The FDM as a material extrusion AM process has gained popularity due to the limitless and simple design possibilities it provides in comparison to traditional manufacturing. To carry out this research and bring to life the various isogrid LCS structure configurations intended for testing, an Anet A6 3D printer was used. The main characteristics of the 3D printer are listed in the following Table 1. The PLA material from the filament manu-

facturer BeeVeryCreative was chosen because it is inexpensive, readily available, easy to print in great quality, and biodegradable; additionally, its mechanical behavior meets the requirements and purposes of this analysis (see Table 2).

**Table 1.** Main specifications of the Anet A6 3D printer used to print the isogrid LCS structure samples.

Layer thickness [mm]	0.1–0.3
Printing speed [mm/s]	10–120
XY axis position accuracy [mm]	0.012
Z axis position accuracy [mm]	0.004
Printing material	ABS, PLA, ...
Filament diameter [mm]	1.75
Nozzle diameter [mm]	0.4 (can be changed)
Build size [mm <sup>3</sup> ]	220 × 220 × 240
File format	STL, G-Code, OBJ

**Table 2.** Main specifications and properties of the BeeVeryCreative PLA 3D printer filament.

Diameter [mm]	1.75 ± 0.05
Printing temperature [°C]	205 ± 10
Specific weight [g/cm <sup>3</sup> ]	1.24
Tensile modulus [MPa]	3120
Yield strength [MPa]	70
Ultimate strength [MPa]	N/A
Strain at break [%]	20
Strain at yield [%]	5
Glass transition [°C]	57

Obviating the details of the initial process relative to the printer adjustments and setup, the printing (or slicing) direction was chosen with the cylinder in the upright position, so that the material anisotropy is kept simple to understand and all the successive layers are printed exactly the same way along the LCS structure with the axis of slicing aligned with the direction of the compressive loading. The Ultimaker Cura slicing software was initially used, but despite attempts to optimize printing performance without printing supports by adjusting the printing parameters, these efforts failed to resolve the existing issue of suspended material and unsatisfactory results caused by still-hot material not remaining in the proper filling by gravity. Another option was to print the LCS structure horizontally, but this resulted in even worse results. To address the issue, an attempt was made to model auxiliary geometry by introducing artificial bridging supports between the auxiliary and the real geometry, thereby improving material separation, but without success. Finally, we investigated the market for software slicers, and after experimenting with several programs that included support material, we obtained excellent results with Simplify3D, where material usage was minimized and the finished product was quite acceptable from a macroscopic standpoint. One example of a printing failure and a successful one with and without the support material are shown in Figure 3.

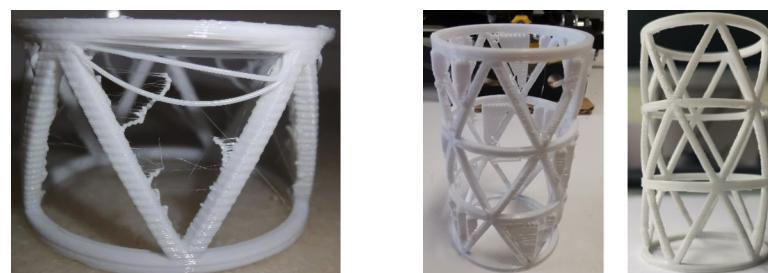


**Figure 3.** 3D printing failed attempt with suspended material (left); successful 3D printing solution using optimized supports generated in Simplify3D with (middle) and without (right) support material.

#### 4. Compressive Testing and Results

As mentioned previously, one of the objectives of this research is to determine whether representative reduced-scale models of large isogrid LCS structures can accurately simulate their mechanical behavior under compressive loads and observe their local buckling behavior. As a result, it was decided to conduct compression tests using four distinct configurations, as illustrated in Figure 5, where the diverse morphologies were chosen to investigate the effect of the length, symmetry, proximity to the applied compressive load, and border effects on the local buckling behavior.

Three samples of each configuration were printed randomly, yielding a total of 12 samples in total; they were tested, also randomly, to avoid systematic errors inherent in the AM process and testing procedures. The final printer settings and configurations were as follows: nozzle diameter = 0.4; infill = 100%; layer height = 0.2 mm; nozzle temperature = 200 °C; build platform temperature off; printing speed = 45 mm/s; and cooling off. The total printing times for all the test samples was 12 h and 12 min; detailed information of this and the geometric description of the samples are listed in Table 3 by type of configuration. Due to time constraints, the printing head velocity was increased. As such, a slight vibration of the printer was observed in some of its displacement trajectories during printing, which may have exacerbated the samples' material and geometric inhomogeneity and reproducibility, possibly resulting in significant interference with the final results, as will be seen.

**Table 3.** Geometric description of the samples, post-processed characteristics, and printing time (simulation and real) for each configuration.

Configuration	$a$ [mm]	$e$ [mm]	$D$ [mm]	$n_h$ #	$n_c$ #	$L$ [mm]	Mass [g]	Rib Length [mm]	Rib Section [mm <sup>2</sup> ]	Printing Time	
										Sim. [min]	Real [min]
A	1.6	2.4	40	10	4	66.90	5.58	20.17	3.84	55	87
B					3	45.13	3.91			37	59
C					2	23.37	2.24			19	30
D					4*	47.13	4.50			41	68

\*: not generated automatically.

The compression tests were conducted using a compression test rig on a universal mechanical testing machine, model Shimadzu AG-X Plus 100 kN (Figure 4). The test speed was set to 0.25 mm/min, and data on both head displacement and applied force were collected at a 50 Hz rate. The tests were conducted in a random order to minimize systematic errors, and the results for the various tests are shown in Figure 5 for the 12 samples. As can be seen from the results, the four configurations support a range of critical compressive loads, suggesting that local buckling cannot be used to accurately predict strength and that a coupling effect exists between global compressive deformation and local buckling effects. As expected, given that all stages have equal stiffness, serial springs (stiffnesses) displacements sum up and the same force is applied to all the unit cell cylinder stages (i.e., with only one triangle along the longitudinal axis); as the stages between two circumferential ribs are piled up, we observe experimentally that the displacement increases almost proportionally, disregarding outliers, as we progress through configurations A, B, and C. The A configuration has the lowest strength, possibly because the local to global buckling coupling is more pronounced due to its length and higher global slenderness. The B configuration has the higher strength, most likely due to the longitudinal rib arrangement and reinforcing central circumference ring, whereas the D and C configurations have slightly lower strength than B. The results suggest that the local-to-global coupling has a greater effect on compressive strength than the local effect of reinforcement and different rib topologies at the load-applied border surfaces.

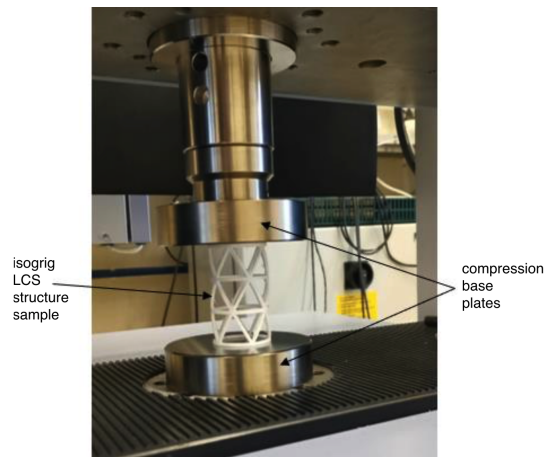


**Figure 4.** Compression testing apparatus.

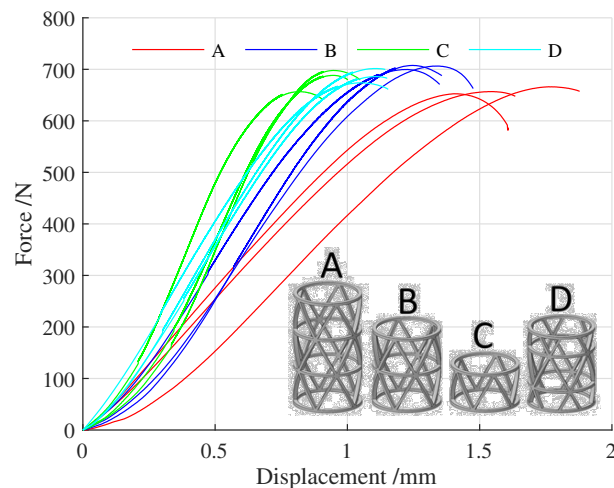


**Figure 5.** Compression test results for the 4 different configurations.

## 5. Conclusions

The purpose of this article is to demonstrate the feasibility of using fused deposition modeling (FDM) technology to fabricate polymer isogrid lattice cylindrical shell (LCS) structures with equilateral triangular unit cells using non-professional and conventional 3D printing software and hardware, and to infer experimentally about local buckling behavior. For these structures, a parametric and automated 3D model was created in SolidWorks using the Visual Basic (VBA) programming language. Due to the geometric complexity of isogrid LCS structures, they were realized through a progressive 3D printing trial-and-error improvement process that included progressive parameter adjustment and a better choice of slicing software to automatically generate 3D printing material supports. The printer's total run time has always been greater than the slicer program simulator's, typically by around 60%. As previously stated, the simulator does not account for extruder heating time, and the speed at which the lines of code execute on the printer varies, so speeds must be adjusted (printing assuming varied movements) to equalize these values and thus obtain a valid time simulation.

To improve control over the final mechanical properties and local buckling behavior repeatability, sensitivity analysis could have been conducted to examine printing parameters such as printing speed, layer height, extruder diameter, and printing temperature (statistical DoE approach). However, the trial and error method used, combined with the use of Simplify3D to generate trajectories and material supports, appears to be a successful strategy to produce isogrid LCS structures with satisfactory quality and compressive strength-to-mass performance. Concerning the compression testing of the various configu-

rations, the print head speed was likely set too high, resulting in a significant discrepancy in results between the three samples of the same configuration. Although the maximum critical compression load and strength are less dispersed, the results indicate that additional research is necessary to determine the exogenous effects impacting local buckling behavior and printing quality. This preliminary study suggests that the order of dispersion of the obtained results precludes a detailed analysis of the sensitivity of various printing parameters using a DoE approach, at least until manufacturing and testing repeatability are improved, as the expected sensitivity of these parameters may be of the same order of magnitude as the obtained result's dispersion. Following this initial approach, more refined subsequent studies will focus on reducing result dispersion by ensuring reduced anisotropy and increased material homogeneity, conducting formal DoE sensitivity analyses to printing parameters, and validating the results using numerical and analytical structural modeling for better understanding of local buckling and global deformation. Nonetheless, this study demonstrates a previously unknown sensitivity of compressive strength to configuration, here denoted as local-to-global buckling coupling, implying that the analytic formulations for the critical local buckling load determination used by Vasiliev and Totaro should be used with caution, a behavior that will be further investigated in future studies, at least for structures with low-order number of helical ribs and cylindrical stages.

**Author Contributions:** Conceptualization, C.M.A.V.; methodology, C.M.A.V. and A.M.S.C.; software, F.C.G.; validation, C.M.A.V. and F.C.G.; formal analysis, C.M.A.V. and A.M.S.C.; investigation, C.M.A.V., F.C.G. and A.M.S.C.; resources, C.M.A.V., F.C.G. and A.M.S.C.; data curation, F.C.G.; writing—original draft preparation, C.M.A.V. and F.C.G.; writing—review and editing, C.M.A.V.; visualization, C.M.A.V. and A.M.S.C.; supervision, C.M.A.V. and A.M.S.C. All authors have read and agreed to the published version of the manuscript.

**Funding:** The authors gratefully acknowledge the support provided by the Foundation for Science and Technology (FCT) of Portugal, within the scope of the project of the Research Unit on Materials, Energy and Environment for Sustainability (proMetheus), Ref. UID/05975/2020, financed by national funds through the FCT/MCTES.

**Data Availability Statement:** Not applicable.

**Conflicts of Interest:** The authors declare no conflict of interest.

## References

1. Huybrechts, S.; Hahn, S.E.; Meink, T. Grid stiffened structures: A survey of fabrication, analysis and design methods. In Proceedings of the 12th International Conference on Composite Materials (ICCM/I2), Paris, France, 5–9 July 1999; p. 10.
2. Vasiliev, V.; Barynin, V.; Razin, A. Anisogrid composite lattice structures—Development and aerospace applications. *Compos. Struct.* **2012**, *94*, 1117–1127. [[CrossRef](#)]
3. Abad, E.M.K.; Pasini, D.; Cecere, R. Shape optimization of stress concentration-free lattice for self-expandable Nitinol stent-grafts. *J. Biomech.* **2012**, *45*, 1028–1035. [[CrossRef](#)] [[PubMed](#)]
4. Beyi, A.F.M.; Ismail, A.E.; Taib, I.; Ibrahim, M.N. Stent classifications and effect of geometries on stent behaviour using finite element method. *Int. J. Mech. Eng. Robot. Res.* **2020**, *9*, 329–340. [[CrossRef](#)]
5. Morozov, E.; Lopatin, A.; Nesterov, V. Finite-element modelling and buckling analysis of anisogrid composite lattice cylindrical shells. *Compos. Struct.* **2011**, *93*, 308–323. [[CrossRef](#)]
6. Lai, C.; Wang, J.; Liu, C. Parameterized Finite Element Modeling and Buckling Analysis of Six Typical Composite Grid Cylindrical Shells. *Appl. Compos. Mater.* **2014**, *21*, 739–758. [[CrossRef](#)]
7. Belardi, V.; Fanelli, P.; Vivio, F. Structural analysis and optimization of anisogrid composite lattice cylindrical shells. *Compos. Part Eng.* **2018**, *139*, 203–215. [[CrossRef](#)]
8. Meyer, R.R.; Harwood, O.P.; Harmon, M.B.; Orlando, J.I. *Isogrid Design Handbook*; NASA Technical Report CR-124075; NASA Marshall Space Flight Center: Huntsville, AL, USA, 1973.
9. De Nicola, F.; Totaro, G.; Lenzi, F.; Ferrigno, A. Mechanical properties of composite anisogrid shell structures. In Proceedings of the 59th International Astronautical Congress, Glasgow, SCT, UK, 9 September–3 October 2008; Number IAC-08.C2.4.4.
10. Totaro, G.; Gürdal, Z. Optimal design of composite lattice shell structures for aerospace applications. *Aerosp. Sci. Technol.* **2009**, *13*, 157–164. [[CrossRef](#)]
11. Totaro, G. Multilevel Optimization of Anisogrid Lattice Structures for Aerospace Applications. Ph.D. Thesis, Delft Technical University, Delft, NL, USA, 2011.

12. Buragohain, M.; Velmurugan, R. Study of filament wound grid-stiffened composite cylindrical structures. *Compos. Struct.* **2011**, *93*, 1031–1038. [[CrossRef](#)]
13. Fan, H.; Fang, D.; Jin, F. Mechanical properties of lattice grid composites. *Acta Mech. Sin.* **2008**, *24*, 409–418. [[CrossRef](#)]
14. Zhang, Y.; Xue, Z.; Chen, L.; Fang, D. Deformation and failure mechanisms of lattice cylindrical shells under axial loading. *Int. J. Mech. Sci.* **2009**, *51*, 213–221. [[CrossRef](#)]
15. Vasiliev, V.; Barynin, V.; Rasin, A. Anisogrid lattice structures—Survey of development and application. *Compos. Struct.* **2001**, *54*, 361–370. [[CrossRef](#)]
16. Vasiliev, V.; Razin, A. Anisogrid composite lattice structures for spacecraft and aircraft applications. *Compos. Struct.* **2006**, *76*, 182–189. [[CrossRef](#)]
17. Del Olmo, E.; Grande, E.; Samartin, C.R.; Bezdenejnykh, M.; Torres, J.; Blanco, N.; Frovel, M.; Canas, J. Lattice structures for aerospace applications. In Proceedings of the 12th European Conference on Spacecraft Structures, Materials and Environmental Testing, Noordwijk, NL, USA, 20–23 March 2012; Ouwehand, L., Ed.; ESA SP-691; European Space Agency: Paris, France, 2012; p. 6.
18. Giusto, G.; Totaro, G.; Spena, P.; Nicola, F.D.; Caprio, F.D.; Zallo, A.; Grilli, A.; Mancini, V.; Kiryenko, S.; Das, S.; et al. Composite grid structure technology for space applications. *Mater. Today Proc.* **2021**, *34*, 332–340. [[CrossRef](#)]
19. Azarov, A.V. Theory of composite grid shells. *Mech. Solids* **2013**, *48*, 57–67. [[CrossRef](#)]
20. Vasiliev, V. *Advanced Mechanics of Composite Materials and Structures*; Elsevier: Amsterdam, NL, USA, 2018.
21. Beerhorst, M.; Hühne, C. Optimization of axially compressed cylindrical grid structures using analytical and numerical models. *Compos. Struct.* **2016**, *157*, 155–162. [[CrossRef](#)]
22. Abbasi, M.; Ghanbari, J. A comprehensive analytical model for global buckling analysis of general grid cylindrical structures with various cell geometries. *Int. J. Comput. Methods Eng. Sci. Mech.* **2021**, *22*, 477–499. [[CrossRef](#)]
23. Totaro, G. Local buckling modelling of isogrid and anisogrid lattice cylindrical shells with triangular cells. *Compos. Struct.* **2012**, *94*, 446–452. [[CrossRef](#)]
24. Delgado, X.M.; Merrett, C.G. Examination of the isotropy assumption in isogrid structures through analysis of nine isogrid variations. In *AIAA Scitech 2021 Forum*; American Institute of Aeronautics and Astronautics: Reston, VA, USA, 2021; p. 19. [[CrossRef](#)]
25. Challis, V.J.; Xu, X.; Zhang, L.C.; Roberts, A.P.; Grotowski, J.F.; Sercombe, T.B. High specific strength and stiffness structures produced using selective laser melting. *Mater. Des.* **2014**, *63*, 783–788. [[CrossRef](#)]
26. Maskery, I.; Aboulkhair, N.; Aremu, A.; Tuck, C.; Ashcroft, I. Compressive failure modes and energy absorption in additively manufactured double gyroid lattices. *Addit. Manuf.* **2017**, *16*, 24–29. [[CrossRef](#)]
27. Li, M.; Lai, C.; Zheng, Q.; Han, B.; Wu, H.; Fan, H. Design and mechanical properties of hierarchical isogrid structures validated by 3D printing technique. *Mater. Des.* **2019**, *168*, 107664. [[CrossRef](#)]
28. Ji, B.; Han, H.; Lin, R.; Li, H. Failure modes of lattice sandwich plate by additive-manufacturing and its imperfection sensitivity. *Acta Mech. Sin.* **2019**, *36*, 430–447. [[CrossRef](#)]
29. Guo, Y.; Yang, H.; Lin, G.; Jin, H.; Shen, X.; He, J.; Miao, J. Thermal performance of a 3D printed lattice-structure heat sink packaging phase change material. *Chin. J. Aeronaut.* **2021**, *34*, 373–385. [[CrossRef](#)]
30. Cao, X.; Ji, B.; Li, Y.; An, X.; Fan, H.; Ke, L. Multi-failure analyses of additively manufactured lattice truss sandwich cylinders. *Compos. Part Eng.* **2021**, *207*, 108561. [[CrossRef](#)]
31. Mancia, F.; Marchetti, M.; Regi, M.; Lionetti, S.; Marranzini, A.; Mazza, F.; Coluzzi, P.; Centro, C.; Materiali, S. Development of 3D advanced rapid prototyping multipurpose structures with micro and nano materials. In *Cost Effective Manufacture via Net-Shape Processing*; Meeting Proceedings RTO-MP-AVT-139; RTO: Neuilly-sur-Seine, France, 2006; Paper 20, pp. 20–1–20–24.
32. Ananth, S.; Whitney, T.; Toubia, E. Buckling stability of additively manufactured isogrid. In Proceedings of the 33rd Technical Conference of the American Society for Composites, Seattle, WA, USA, 24 September 2018; DEStech Publications, Inc.: Lancaster, PA, USA, 2018; Volume 5, pp. 3180–3193. [[CrossRef](#)]
33. MacDonald, E.; Espalin, D.; Doyle, D.; Muñoz, J.; Ambriz, S.; Coronel, J.; Williams, A.; Wicker, R. Fabricating patch antennas within complex dielectric structures through multi-process 3D printing. *J. Manuf. Process.* **2018**, *34*, 197–203. [[CrossRef](#)]
34. Forcellese, A.; Simoncini, M.; Vita, A.; Pompeo, V.D. 3D printing and testing of composite isogrid structures. *Int. J. Adv. Manuf. Technol.* **2020**, *109*, 1881–1893. [[CrossRef](#)]
35. Forcellese, A.; di Pompeo, V.; Simoncini, M.; Vita, A. Manufacturing of isogrid Compos. Struct. by 3D printing. *Procedia Manuf.* **2020**, *47*, 1096–1100. [[CrossRef](#)]
36. Velasco-Hogan, A.; Xu, J.; Meyers, M.A. Additive manufacturing as a method to design and optimize bioinspired structures. *Adv. Mater.* **2018**, *30*, 1800940. [[CrossRef](#)]
37. Reddy, A.H.; Davuluri, S.; Boyina, D. 3D printed lattice structures: A brief review. In Proceedings of the IEEE International Conference on Nanomaterials: Applications & Properties (NAP-2020), Sumy, Ukraine, 9–13 November 2020; IEEE: Piscataway, NJ, USA, 2020; p. 5. [[CrossRef](#)]
38. Budynas, R.G.; Nisbett, K.J. *Shigley's Mechanical Engineering Design*, 11th ed.; McGraw-Hill Education: New York, NY, USA, 2020; pp. 207–210.